

NACA RM No. E8G01

CLASSIFICATION                      CHANGED

~~RESTRICTED UNCLASSIFIED~~ *by auth H.L. Dryden  
per each release  
form 1576-4/13/53  
dkt 5/20/53*

**NACA**

C.2

by authority of *H.L. Dryden per NACA Release*  
*form 740 dated 3-10-52.*  
*By HHR, 4-11-52.*

# RESEARCH MEMORANDUM

PERFORMANCE OF 24-INCH SUPERSONIC AXIAL-FLOW COMPRESSOR IN AIR

## II - PERFORMANCE OF COMPRESSOR ROTOR AT EQUIVALENT TIP SPEEDS FROM 800 TO 1765 FEET PER SECOND

By Irving A. Johnsen, Linwood C. Wright, and Melvin J. Hartmann .

**Lewis Flight Propulsion Laboratory  
Cleveland, Ohio**

CLASSIFIED DOCUMENT

This document contains classified information affecting the National Defense of the United States within the meaning of the Espionage Act, USC 50:91 and 92. Its transmission or the revelation of its contents in any manner to an unauthorized person is prohibited by law. Information so classified may be imparted only to persons in the military and naval services of the United States, appropriate civilian officers and employees of the Federal Government who have a legitimate interest therein, and to United States citizens of known loyalty and discretion who of necessity must be informed thereof.

## NATIONAL ADVISORY COMMITTEE FOR AERONAUTICS

WASHINGTON  
January 21, 1949

RESTRICTED

NACA RM No. E8G01



3 1176 01435 5458

NATIONAL ADVISORY COMMITTEE FOR AERONAUTICS

RESEARCH MEMORANDUM

PERFORMANCE OF 24-INCH SUPERSONIC AXIAL-FLOW COMPRESSOR IN AIR

II - PERFORMANCE OF COMPRESSOR ROTOR AT EQUIVALENT TIP

SPEEDS FROM 800 TO 1765 FEET PER SECOND

By Irving A. Johnsen, Linwood C. Wright  
and Melvin J. Hartmann

SUMMARY

As part of the NACA research program on supersonic axial-flow compressors, a 24-inch-diameter rotor has been **designed**, constructed, and investigated in air up to an actual tip **speed** of 1654 feet per second **and** a maximum equivalent tip speed of 1765 feet per second. This rotor is aerodynamically similar to the supersonic rotor that was **run at approximately the same Mach number and about one-half** the actual tip speed in **Freon-12** at the NACA Langley Aeronautical laboratory. Analysis of the experimental data is **made with regard** to the theoretical performance, particular attention **being focused** on the problem of diffusion in the **rotor** passages. The effect of the existence of **pressures** in the rotor requiring radial velocities for equilibrium is discussed and the necessity of a close approach to simple equilibrium after the shock is indicated.

The maximum pressure ratio produced in the single stage without inlet guide vanes **was** 2.08 at 1765 feet per second and was obtained at an adiabatic efficiency of 0.79 and a **weight** flow of 64.0 lb per second. The general performance closely paralleled that obtained in the Langley investigation in Freon-12.

50,000  
E.F.M.

**Performance** measurements indicated that theorized **supersonic-**compressor performance **characteristics were** closely approached but not fully achieved at the equivalent tip speed of 1765 feet per **second**.

~~RESTRICTED~~  
RESTRICTED

## INTRODUCTION

A program of research on axial-flow compressors operating with supersonic velocities relative to the rotor blades is being conducted by the NACA. The first part of this investigation, including supersonic-diffuser studies (reference 1), cascade studies, and the design and operation of an experimental compressor in Freon-12 (references 2 and 3), was conducted at the NACA Langley Aeronautical laboratory.

A second phase of this program was conducted at the NACA Lewis laboratory to achieve full-speed operation of a supersonic compressor in air and to confirm, in air, the performance obtained in Freon-12 (dichlorodifluoromethane ( $\text{CCl}_2\text{F}_2$ ), a commercial refrigerant). A rotor was constructed that was aerodynamically similar to the rotor of reference 3 but with the structural design refined to allow design-speed operation in air. The investigation is being conducted in a variable-component supersonic-compressor unit that was built for full-scale supersonic-compressor research. Performance results in air at the design equivalent tip speed of 1600 feet per second, as well as a description of the rotor and the apparatus, are given in reference 4.

The original design of the supersonic compressor differed from the compressor of the present investigation in three respects:

1. The original design contained inlet guide vanes.
2. The original design utilized hub and tip wall curvature.
3. The original design had its minimum thickness increased by 50 percent for the present design.

The combination of  $\theta$  and curvatures was intended to give the spanwise static-pressure distribution behind the normal shock required for simple equilibrium at that point. This design resulted in an almost constant value of blade relative inlet Mach number and total pressure along the blade span.

The experimental results of the first configuration indicated severe separation at the blade tip. In an effort to relieve the separation several changes were made. The hub and tip wall curvature was eliminated after the rotor, and the blade outlet annulus was restricted with good results (reference 3). The tip total pressure was then increased by elimination of the inlet guide vanes, which through prerotation of the tip flow reduced the tip relative total pressure. At the same time, the inlet hub and tip wall curvature was also eliminated. Each of the first two changes made at

the Langley laboratory and the third made at the Lewis laboratory resulted in improved performance. This investigation in air was therefore made without inlet guide vanes or hub and tip wall curvature.

In Order to reduce the vibratory stress in rotor blades to an acceptable level, as discussed in reference 4, it was found necessary to increase the minimum percentage thickness of the original design by 50 percent.

The performance for the modified supersonic-compressor rotor operating without inlet guide vanes over the range of equivalent tip speeds from approximately 800 to 1765 feet per second are presented.

#### Symbols

The following symbols are used in the evaluation of compressor performance:

- A area, (sq ft)
- a local velocity of sound, (ft/sec)
- $a_s$  velocity of sound based on original stagnation conditions, (ft/sec)
- g acceleration due to gravity, 52.174 (ft/sec<sup>2</sup>)
- M absolute Mach number, ratio of absolute air velocity to local velocity of sound
- M' relative Mach number, ratio of air velocity relative to rotor to local velocity of sound
- $M_c$  compressor Mach number,  $U_t/a_{s,1}$
- n rotor speed, (rps)
- P total, or stagnation, pressure of absolute air, (lb/sq ft)
- P' total, or stagnation, pressure of air relative to rotor, (lb/sq ft)
- P static, or stream, pressure, (lb/sq ft)

- R gas constant for normal air, 53.50 (ft-lb)/(lb)(°F)
- r compressor radius, ft
- T total, or stagnation, temperature, (°R)
- t static, or stream, temperature, (°R)
- U velocity of rotor ( $2\pi rn$ ) at radius  $r$ , (ft/sec)
- V absolute air velocity, (ft/sec)
- V' air velocity relative to rotor, (ft/sec)
- W **weight** flow, (lb/sec)
- z distance along axis, (ft)
- $\beta$  angle between compressor axis and absolute air velocity, (deg)
- $\beta'$  angle between compressor axis and air velocity relative to rotor, (deg)
- $\gamma$  ratio of specific heats for normal air, 1.40
- $\delta$  ratio of actual inlet total pressure to standard sea-level pressure,  $P_1/2116$
- $\eta_{ad}$  adiabatic efficiency
- $e$  ratio of actual inlet stagnation temperature to standard **sea-** level temperature,  $T_1/518.4$
- $\rho$  density, (lb/cu ft)
- Subscripts:
- 1 compressor **inlet**
- 2 rotor inlet
- 5 rotor outlet (survey measuring station)
- 6 rake measuring station
- cr conditions at critical speed of sound ( $M = 1.0$ )

**r** radial component  
**T** temperature-rise basis  
**t** tip  
**W** weight-flow **average**  
**Z** axial component, **distance** along the **axis**, (ft)  
**e** tangential component

The vectors defined in the symbols are **illustrated** in figure 1.

### PROCEDURE

The **compressor** was investigated over the range of equivalent tip speeds  $U_t/\sqrt{\theta}$  from 797 to 1608 feet per second with inlet air induced **from** the test cell at temperatures from 77° to 87° F. **In** order to obtain an equivalent tip speed of 1765 feet per **second**, the compressor was operated with refrigerated inlet **air at** a temperature of approximately -15° to -20° F. The maximum actual tip speed attained was 1634 feet per second. Data were taken as described in reference 4, with air flow varied from wide-open throttle to stall.

Although three adiabatic-efficiency terms were presented in reference 4, the adiabatic efficiency  $\eta_{ad,T}$  based on a **weight-flow** average of total-pressure ratio and an **area** average of temperature rise was found to provide the most consistent and **accurate** evaluation of the efficiency of compression. **The  $\eta_{ad,T}$  term is therefore used in the presentation of performance results.**

Weight flow determined from orifice measurements and a weight-flow-average total-pressure ratio  $(P_5/P_1)_W$  measured at the survey station as defined in reference 4 are also used in the presentation of compressor **performance**.

In order to **determine** the **angle** of the air with respect to the **rotor** blades at the inlet, determination of the **axial** velocity of the air immediately ahead of the rotor is **necessary**. The average **axial Mach numbers and the air angles were therefore calculated** on the basis of weight flow, total pressure, and temperature in the inlet section of the rig. This calculation **assumes (1)** an isentropic change through the inlet section, (2) a constant **axial** velocity across the **annulus with** no boundary layer, and (3) no **prerotation** of the air. The inlet mock-up studies discussed in reference 4 indicated that

the first two assumptions could be made with very little error. Also, the mean prerotation is probably small and can be **neglected**. The Mach numbers **and air angles calculated on** this basis represent **an** approximate condition across the passage **and** do not show local **variations** that might be the result of wave formations ahead of the rotor. The calculated values are, however, indicative of the general inlet characteristics of **the** compressor. **The** details of the method of computing **Mach** numbers and **angles** on **this** basis are given **in the** appendix.

Another method of determining the axial Mach numbers at the rotor **inlet** in the absence of **a** survey tube is to assume **a linear** variation in static pressure between the root **and** tip **wall** taps and no loss in total pressure through the **inlet** section. **These** calculated **Mach** numbers were considered to be rather inaccurate, however, because they are **sensitive** to small **static-pressure** changes (particularly at low inlet pressures) **and** because the wall-tap **static-pressure readings** were affected by local surface **irregularities**. **In general**, the difference between the static pressures measured at root and tip was small but considerable discrepancy existed between the orifice weight flow and an integrated weight flow based on this type of calculation. This **method** was therefore not **used** to determine rotor-inlet **angles**.

Conditions at the rotor outlet are **determined** from the survey measurements **as described** in reference 4. These measurements along with rotor speed are sufficient to define total pressure, relative and absolute air angles, and relative and absolute Mach numbers at the rotor outlet. Details of calculation are given in the appendix.

## RESULTS AND DISCUSSION

### Over-All Performance

Over-all **performance** characteristics are given for the **24-inch** supersonic rotor operating in air without guide vanes. These results are then **compared** with those obtained **in Freon-12** as presented in reference 3.

Performance characteristics in air. - The curves of  $(P_5/P_1)_W$  as a function of equivalent weight flow  $W\sqrt{\theta}/\delta$  with superimposed contours of adiabatic efficiency  $\eta_{ad,T}$  are shown in figure 2 for equivalent tip speeds from 797 to 1765 feet per second. **Maximum** total-pressure ratios produced **in the single stage varied** from 1.18 at 797 feet per second to 2.08 at 1765 feet per second; a

total-pressure ratio of 1.93 was obtained at the design speed of approximately 1600 feet per second. The equivalent weight flow at maximum total-pressure ratio was 58.12 and 64.07 pounds per second at rotor tip speeds of 1608 and 1765 feet per second, respectively. These weight flows are less than predicted by the theory that supersonic flow enters parallel to the rearward side of the blades near the leading edge. The difference was approximately 10 percent at 1608 feet per second and 3.5 percent at 1765 feet per second for the rotor operating without inlet guide vanes.

A maximum efficiency of 0.84 was obtained at an impeller tip speed of 797 feet per second (fig. 2). The maximum efficiency decreased to 0.79 and remained essentially constant in the speed range from 1400 to 1765 feet per second. In this range, as hypothesized in reference 3, the expected drop in shock efficiency due to increased Mach number is apparently compensated for by the corresponding decrease in wave losses as the bow waves come closer to attachment and finally form a normal shock in the inlet passage.

The efficiency contours over the speed range illustrate a characteristic difference between a subsonic and a supersonic-axial-flow-compressor stage. In a subsonic-compressor stage, an efficiency less than the maximum value occurs at two distinct mass flows because of the existence of an optimum angle of attack on the blade at a flow intermediate between the flow limits. For a given blade Mach number in the supersonic speed range, however, the classic supersonic compressor with passage-contained shock has a continually increasing efficiency up to the maximum value, which occurs at the maximum pressure ratio. The limiting operating condition is reached, of course, when the passage-contained shock is forced out ahead of the blading and stall or spillage occurs. A transition to constant mass flow and a singularity of efficiency points takes place in the transonic speed range. These characteristics may be considered fundamental manifestations of the diminishing range of blade angle of attack as the supersonic conditions are approached or a transition from blade flow to passage flow. The curves of figure 2 indicate a subsonic characteristic up to a rotor tip speed of approximately 1200 feet per second and a tendency for peak efficiency to move closer to peak total-pressure ratio as speed is increased.

At rotor tip speeds from 1399 to 1765 feet per second, the performance corresponds to that obtained in supersonic diffusers and to that predicted from fundamental supersonic-passage flow theory; that is, maximum efficiency occurs at peak pressure ratio. True supersonic-flow characteristics (no variation of weight flow with an increase in back pressure, as well as the singularity of efficiency points) are approached as speed is increased (fig. 2).



Comparison with characteristics in Freon-12. - In the Freon-12 studies of reference 3, true supersonic-flow characteristics (as defined by the variation in mass flow with change in back pressure) were more closely approached, and the transition from subsonic to supersonic characteristics was more rapid than in this air investigation without inlet guide vanes. This slowness of transition is probably the result of the wide variation in inlet Mach number that exists across the annulus without inlet guide vanes. Although the three-dimensional aspects of the problem are not fully understood, supersonic flow probably first enters the rotor in the region of high relative Mach number at the rotor tip and the attachment of the bow wave progresses along the blade toward the root as speed is increased. The effect of progressive entry of shock was minimized in the Freon-12 investigation because the guide vanes provided a nearly constant value of Mach number across the inlet annulus. Furthermore, the entry of shock across the entire annulus could be attained at a lower rotative speed with the inlet guide vane5 because the vanes increased the relative Mach number at the blade root.

The curves of figure 3 show the comparative values of maximum total-pressure ratio as a function of compressor Mach number and the corresponding equivalent tip speed in air for the Freon-12 investigation of reference 3 and for the air investigation. The pressure-ratio curves have a parallel trend throughout the speed range with the values for the air investigation higher than those of the Freon-12 investigation throughout. The difference in the absolute values can probably be attributed to a combination of the following effects:

1. Operating without inlet guide vanes reduces the relative Mach number at the root and increases it at the tip of the rotor.

2. Because of the difference in physical properties between air and Freon-12, the relative inlet Mach number  $M'_2$ , which is  $V'_2/a_2$ , is higher in air than in Freon-12 for the same compressor Mach number  $M_c$ , which is  $U_t/a_{s,1}$ .

3. The rotor used in this investigation was machined to closer tolerances than the fabricated rotor of reference 3, which reduced the variation in performance from passage to passage and thereby improved over-all performance.

4. The increase in blade thickness and therefore contraction ratio that was incorporated in this rotor increases the efficiency of shock recovery at a given relative Mach number when the shock is contained in the passage.

A **quantitative independent** evaluation Of **each of these factors** is impossible. **The effect Of each of the last three items, however,** would be **to increase the pressure ratio, whereas the first** probably has only a small effect on the **average pressure ratio of the compressor.** **In view of the existing physical differences the maximum pressure-ratio data obtained in air are therefore considered to constitute a substantiation Of the results Of reference 3.**

In this investigation, **as in the Langley program, a smooth transition** from subsonic to supersonic flow **was observed** as the compressor **was accelerated** (fig. 3). As discussed in **reference 2,** it can be hypothesized that, **in accelerating the compressor,** attachment of the bow waves to form a normal shock within the passage would produce no sudden effect on observed performance. Furthermore, in this compressor, the attachment of shock probably progresses down the **blade as speed is increased, as previously mentioned, and the three-dimensional aspects of the flow probably obscure the effect of the discontinuities observed when shock is swallowed in supersonic diffusers.**

The experimental results obtained in the present investigation **have shown the general supersonic theory as applied to supersonic compressors to be correct and have demonstrated that operation in air is feasible.** **The performance trends, in general, parallel those observed in the Freon-12 investigations of reference 3.**

#### Rotor-Inlet Characteristics

As discussed in **reference 3,** one of the first **inferences** of the **hypothesized supersonic operating theory** is that supersonic **flow enters parallel to the rearward side Of the blades at or near the leading edge.** **Figure 4 shows the pitch-section relative air angle at the blade inlet as a function Of equivalent tip speed for maximum total pressure-ratio points.** **The relative air angle is calculated** as described in the appendix and therefore represents a general rotor-inlet characteristic. A **comparison Of the relative-air-angle curve with the physical blade angle** shows that the **condition of parallel entry was approached but not achieved as the rotor speed was increased.** **The difference at an equivalent tip speed of 1765 feet per second was of the order of that found for supersonic operation in the Langley investigation (reference 3).** **The condition of true supersonic operation, with the rotor-inlet angle independent Of rotational speed and throttle position, was not achieved in the 58 run 5 without inlet guide vanes.** **Supersonic operation across the entire annulus however, was probably closely**

approached at an equivalent tip speed of 1765 feet per second, as was indicated by the following conditions:

1. The condition of no change in weight flow with an increase in back pressure was very nearly reached.
2. The relative air angle approached the physical angle of the rearward side of the blade at the inlet.
3. The relative Mach number at the root was very nearly equal to that required for attachment of shock to the  $10^\circ$  wedge; that is, the condition where shock would become attached across the entire inlet span of the blade was just being reached.
4. At equivalent tip speeds of 1508 and 1608 feet per second, the existence of a detached bow wave at the blade root was indicated by a sharp rise in the wall-tap static pressure immediately upstream of the rotor. At an equivalent tip speed of 1765 feet per second, however, this sharp rise in static pressure was not in evidence, indicating that the shock was attached or near attachment at the blade root.

These effects all tend to verify the fact that supersonic operation was just being reached over the entire blade span at an equivalent tip speed of 1765 feet per second corresponding to a compressor Mach number of 1.58.

#### Rotor-Passage Flow Characteristics

The most apparent advantage of supersonic compressors is the large total-pressure ratio per stage. Hence, even though the pressure ratio obtained in this single-stage compressor is greater than has ever been attained in a subsonic axial-flow stage, the discrepancy between theoretical and experimental values requires an explanation. In figure 2, the maximum total-pressure ratio for the design speed of 1600 feet per second is seen to be about 1.93, whereas the design value for the rotor without inlet guide vanes (including only shock losses) is approximately 2.82. Because only part of this discrepancy can be accounted for by the inefficiency of compression, apparently neither the useful work of compression (based on total-pressure ratio) nor the total work of compression (based on temperature rise) is as high as is indicated in theory. In order to determine the reasons for this departure from theory, examination of the nature of flow in the rotor passage is necessary.

1697

**Full information** On the flow **within** the **passages** of the rotor is unavailable **because** of **extreme** difficulty of placing **instrumentation** within rotating passages. **Some** indication of the nature of the flow in the **rotor** may be obtained, however, **from** data **taken** across the rotor-outlet **annulus**. The data for the **maximum** total-pressure condition at an **equivalent** tfp speed of 1608 feet per second **will** be used to **illustrate** passage-flow characteristics, **inasmuch** as these data **are** typical Of operation in the **high-speed** range.

**Useful work of compression.** A plot of the relative Mach number across the rotor-outlet annulus (fig. 5) shows that the **actual** passage-outlet Mach-number **is** high compared to the **average** value Of approximately 0.6 for **which** the outlet **annulus** was designed. This lack of diffusion of the **exit** Mach number **reduces** the total pressure **and** therefore the **useful** work of **compression** because of the **following** three effects:

1. Reduction in **static-pressure** rise within passage caused by **incomplete** diffusion
2. Reduction in kinetic **energy** in **absolute** stream because high relative **Mach** number corresponds to reduced absolute Mach number at passage **outlet** for this **particular** rotor **geometry**
3. Increased **total-pressure** losses due to high Mach number level **in** channel

The **sensitivity** of total-pressure ratio to the **amount** of diffusion in the rotor passage can be seen **from** figure 6. These data **are** calculated for the pitch section at a tip speed of 1600 feet per **second**, with no **losses** considered **except** the normal-shock loss at the **minimum** section. The figure indicates that **proper** diffusion after the shock is **essential** for **maximum** performance of the **compressor**.

Although **the** **fundamental** reason<sup>s</sup> for the incomplete diffusion in the rotor passage **cannot** be **conclusively** Stated, the **following** four conditions contribute to that result:

1. **The** **large** ratio Of Wetted area to **cross-sectional** area allows **a** **large** part of the passage to be taken up with **boundary** layer, which **tends** to **promote** **large** **frictional** losses, **separation**, **and** ineffective subsonic diffusion in the passage after the shock.

2. Interaction of the normal shock with the boundary layer can be **expected** to **thicken** the boundary layer and greatly enhance **sep-** **aration** tendencies. Also the **centrifuging** toward the tip of the low-velocity air on the blade **surfaces** tend<sup>s</sup> to restrict the effective **expansion** area because of the **accumulation** of slowly **moving** air at the tip.

The tendency, even in **smooth nozzles**, for a gradual **pressure rise** to occur near **the passage walls** while the fluid near the **passage center experiences** the normal-shock **pressure rise** also increases the passage-outlet Mach number.

3. Although the effect is not fully understood, a radial flow resulting from a lack of **equilibrium** between **centrifugal** force and pressure after the shock probably acts to **reduce the** amount of passage diffusion. Figure 7(a) shows, for the **maximum** pressure-ratio condition at 1606 feet per second, a plot of the theoretical **static-pressure gradient**  $\frac{dp}{dr}$  that would exist after a normal shock at **the minimum-area section (considering Only shock losses and neglecting equilibrium) as** compared with the approximate static-pressure gradient required for simple radial equilibrium (no radial acceleration, or  $\frac{dp}{dr} = \frac{\rho v_\theta^2}{gr}$ ) after the shock. This appreciable difference shows that **simple radial equilibrium** does not exist. The difference **must** be equal to the **sum of the terms involving** radial motion in the complete equation for radial equilibrium

$$\frac{dp}{dr} = \frac{\rho v_\theta^2}{gr} - \frac{\rho v_z}{g} \frac{\partial v_r}{\partial z} - \frac{\rho v_r}{g} \frac{\partial v_r}{\partial r} \quad (1)$$

If conditions after the shock are **considered** with regard to this more complete equation for radial **balance** of forces, probable influences on the flow path through the **rotor may be** surmised. As in the calculation of figure 7(a), the assumption can be made that in the **absence** of inlet guide vanes: (1) the static-pressure gradient in front of the shock is very nearly zero with little or no radial- or **tangential-velocity** components; and (2) a shock **normal** to this entering streamline occurs at the local Mach number.

Directly after the shock, the static **pressure** gradient  $\frac{dp}{dr}$ , due to variation in relative Mach number **along** the blade, is **considerably** greater than that required for simple equilibrium as shown in figure 7(a). **This difference must then be accounted for** by the terms

involving radial motion  $\left( -\frac{\rho v_z}{g} \frac{\partial v_r}{\partial z} - \frac{\rho v_r}{g} \frac{\partial v_r}{\partial r} \right)$ . With the radial components **before the shock** small and the shock **assumed** to be close to normal,  $v_r$  immediately after the shock is very **small compared** to  $v_z$ . Also, from the **nearly constant difference** between the curves in figure 7(a),  $\partial v_r / \partial r$  will be small. The term  $\frac{\rho v_r}{g} \frac{\partial v_r}{\partial r}$  of equation (1) is therefore **smaller** than  $\frac{\rho v_z}{g} \frac{\partial v_r}{\partial z}$ . Because  $\frac{\rho v_\theta^2}{gr}$  is too

small (fig. 7(a)) and  $V_z$  is positive, the value of  $\frac{\partial V_r}{\partial z}$  must be negative. The streamline must then be concave inward after the shock with the radial velocities increasing toward the root along  $z$ .

From the geometry of the passage, the radial velocity cannot be sustained indefinitely and the streamline must be deflected back toward the axial direction. In this process, the term  $\frac{\rho V_z}{g} \frac{\partial V_r}{\partial z}$  must pass through zero and become positive. This change in sign corresponds to an inflection of the streamline from concave inward to concave outward. As the flow progresses along the axis, the radial component must eventually vanish and the term  $-\frac{\rho V_z}{g} \frac{\partial V_r}{\partial z}$  will again become larger than  $\frac{\rho V_r}{g} \frac{\partial V_r}{\partial r}$ . If this event occurs, from the complete radial equilibrium equation,  $\frac{dp}{dr}$  will be less than the corresponding value of  $\frac{\rho V_\theta^2}{gr}$ .

An examination of the data at the survey Station 0.6 Chord length downstream of the rotor (fig. 7(b)) indicates that this condition exists. Thus, over the greater portion of the annulus simple equilibrium does not exist and there are radial-flow components.

This hypothesis shows that flow is displaced downward from the tip in passing through the rotor, thus reducing the effective area available for the passage of mass flow and consequently reducing the amount of passage diffusion. In addition, the adverse pressure gradients induced at the tip may cause flow separation. The net result indicates that the radial balance of forces must be considered and the radial-flow components must be controlled before optimum flow can be set up in the passage.

Review of the initial assumption of a normal shock is now expedient. The shock most probably does not remain normal to the streamlines because the equilibrium pressures behind the shock do not correspond to those required by the normal-shock relations. The shock therefore warps in a direction that tends to deflect the streamlines radially outward and alter the shock pressure gradient toward that computed for simple equilibrium. Thus, a combination of shock deflection and radial motion will fix the streamline. Determination of the relative magnitude of each effect from the available data is impossible.

Each of these three factors probably contributed to the ineffective diffusion and high relative Mach number in the passage after the shock. In view of the dependence of over-all performance on adequate subsonic diffusion, apparently these effects must be minimized for optimum performance.

The pressure recovery in the rotor passage, determined as described in the appendix, is shown in figure 8 for the maximum-pressure-ratio point at 1608 feet per second. This curve indicates a very high pressure recovery near the rotor root and low recoveries near the tip. Only part of this variation in pressure recovery can be explained on the basis of the variation in normal shock efficiency across the annulus. A radial transfer of energy therefore appears to exist toward the root, probably the result of the lack of equilibrium after the shock and the centrifuging of low-energy air toward the tip.

Total work of compression. - The total energy input to the air may be given by the expression  $U\Delta V_\theta$ , where  $\Delta V_\theta$  may be broken into two parts:

1. The tangential velocity imparted due to reduction in the air velocity relative to the rotor as the result of static-pressure rise in the rotor passage. The static-pressure rise, which has already been discussed, affects both the useful and total work of compression.

2. The tangential velocity imparted due to the stream turning in the direction of rotation that occurs in the rotor passage.

The relative air angles at rotor inlet and outlet are shown in figure 9 for the maximum pressure-ratio condition at 1606 feet per second. Physical blade angles are also plotted to indicate the degree to which air follows the blades. Maximum turning exists at the pitch and is greater than design turning. Both root and tip show less than design turning, with the tip showing reverse turning. Only a slight reduction in work input due to lack of turning relative to the blades exists, although there is some deviation from the local physical blade angle. This condition indicates that the lack of diffusion after the shock is the primary cause of the departure from theoretical total work and useful work of compression.

The tip reverse turning at the design operating condition, which was also encountered in the Freon-12 studies, may be accounted for by a combination of several factors:

1. The possibility of error in **static-pressure measurement** of survey tube exists in region near walls.
2. Flow leakage through tip clearance space probably results in reduced turning.
3. Separation from both convex and concave sides of the blades may be caused by the general instability of the flow along with the centrifuging of low-momentum air toward the *outer shroud*. Early transition and separation has been frequently noted to occur in a diffusing passage following a strong shock. With the **passage turning** washed out in this manner, only small effects 5x8 necessary to create the **reverse turning**.
4. Irrotation of the inlet air establishes a rotation within the blade passage that is opposite to the direction of rotation at the tip and in the direction of rotation at the root. This effect will tend to reduce turning at the tip and increase turning at the root.

#### Rotor-Outlet Characteristics

The variation in total-pressure ratio, absolute axial and tangential Mach number, and absolute air angle across the rotor-outlet passage is shown in figure 10 for the maximum total-pressure-ratio condition at an equivalent tip speed of 1606 feet per second. The decline in both the total-pressure ratio and axial Mach number profiles at the rotor tip exemplifies the effect of centrifugence of the low-velocity air toward the tip and the effects of the radial flow and radial transfer of energy that result at least partly from lack of equilibrium following the shock. Furthermore, the previous comparison of the measured outlet static pressures with the pressure distribution required for equilibrium (based on measured rotational air velocities, fig. 7(b)) indicated that the condition of simple equilibrium has not yet been achieved at the survey station. As previously mentioned, this lack of simple equilibrium apparently exists as a result of the radial accelerations set up because of the nonequilibrium conditions after the blade shock with the adjustment in the flow still taking place at the survey station.

The existence of radial flow will introduce an error in the measured static pressure, thereby affecting the outlet Mach number and velocity values. This effect is probably not large, however, in view of the fact that the weight flow integrated over the rotor-outlet annulus agreed with the orifice measured weight flow within approximately 3 percent.



The absolute air angle  $\beta_5$  (stator stagger angle) is less than design across the entire blade span except at the tip (fig. 10) where effective overturning of the low-momentum air exists as a result of the low axial Mach number in that region.

Extreme gradients are apparent in the turning angle, axial Mach number, and total-pressure-ratio profiles across the rotor outlet. In addition to the immediate losses in rotor performance that result from these extreme variations, it is apparent that the recovery of the kinetic energy at the rotor outlet is a serious problem and design of stator blades to convert this energy to pressure efficiently would be difficult.

### SUMMARY OF RESULTS

The following results were obtained from an investigation of the NACA 24-inch axial-flow supersonic-compressor rotor in air over the equivalent tip speed range from 797 to 1765 feet per second:

1. Maximum pressure ratio produced in the single stage varied from 1.18 at 797 feet per second to 2.06 at 1765 feet per second. The equivalent weight flow at maximum total-pressure ratio was 58.12 pounds per second at the design speed of 1608 feet per second and 64.07 pounds at 1765 feet per second.

2. A maximum efficiency of 0.84 occurred at an equivalent tip speed of 797 feet per second, decreasing to 0.79 for speeds from 1400 to 1765 feet per second.

3. The performance closely paralleled that of the Langley rotor run in Freon-12. The general performance was qualitatively characteristic of the theoretical supersonic compressor, with a subsonic characteristic at low speeds and a transition to a supersonic characteristic taking place in the transonic speed range. In the supersonic range, the variation in efficiency with a change in back pressure was nearly the same as that predicted from theory.

4. Results indicated that true supersonic operation over the entire blade span was being closely approached at the equivalent tip speed of 1765 feet per second.

5. Study of the flow process in the rotor passage indicated that the discrepancies between design pressure ratio, 2.62, and that measured at design speed, 1.93, was due to incomplete passage diffusion, which in turn, was due at least partly to the lack of

simple **equilibrium** directly after **the** normal shock. **Results indi-**  
cat8 that the radial balance of forces must be **considered** and the  
radial-flow components must be controlled before **optimum** flow can  
be **set up** in the passage.

**Lewis Flight** Propulsion Laboratory,  
National Advisory Committee for Aeronautics,  
**Cleveland, Ohio.**

## A P P E N D I X - ~ - COMPUTATION METHODS

Rotor inlet. - The critical-area ratio may be determined by use of the relation

$$W = \rho_{cr} a_{cr} A_{cr}$$

With the **assumption** of no loss in total **pressure** or total **temperature** from station 1-to station 2, the relation can be put in the form

$$\frac{A_2}{A_{cr}} = \sqrt{\frac{\gamma g}{RT_1}} \left| \frac{P_1 A_2}{W \left(\frac{\gamma+1}{2}\right)^{\frac{\gamma+1}{2(\gamma-1)}}} \right|$$

If values for  $\gamma$ , R, and  $g$  are substituted

$$\frac{A_2}{A_{or}} = \frac{0.531 P_1 A_2}{W \sqrt{T_1}}$$

The axial Mach number **is then** found from the relation

$$\left(\frac{A_2}{A_{cr}}\right)^2 = \frac{1}{(M_2)^2} \left\{ \frac{2}{\gamma+1} \left[ 1 + \frac{\gamma-1}{2} (M_2)^2 \right] \right\}^{\frac{\gamma+1}{\gamma-1}}$$

The Solution for  $M_2$  **is** simplified by the **use** of **tables relating** Mach number and area ratio.

**The velocity and Mach number relative to the rotor can then be determined as follows:**

$$P_2 = \frac{P_1}{\left[ 1 + \frac{\gamma-1}{2} (M_2)^2 \right]^{\frac{\gamma}{\gamma-1}}}$$

$$t_2 = \frac{T_1}{\left[ 1 + \frac{\gamma-1}{2} (M_2)^2 \right]}$$

$$a_2 = \sqrt{\gamma R g t_2}$$

and

$$V'_{z,2} = V_2 = M_2 a_2$$

$$V'_{\theta,2} = \frac{r U_t}{r_t}$$

$$\beta'_2 = \tan^{-1} (V'_{\theta,2} / V'_{z,2})$$

Therefore

$$M'_2 = \frac{V'_{z,2}}{\cos \beta_2 a_2} = \frac{M_2}{\cos \beta_2}$$

and

$$P'_2 = P_2 \left[ 1 + \frac{\gamma-1}{2} (M'_2)^2 \right]^{\frac{\gamma}{\gamma-1}}$$

Rotor outlet. - At the rotor outlet, the values of  $P_5$ ,  $P_5$ ,  $\beta_5$ , and  $T_5 (= T_6)$  are determined by direct measurement from which the other absolute values may be calculated:

$$t_5 = T_5 \left( \frac{P_5}{P_5} \right)^{\frac{\gamma-1}{\gamma}}$$

$$a_5 = \sqrt{\gamma R g t_5}$$

$$M_5 = \left\{ \frac{2}{\gamma-1} \left[ \left( \frac{P_5}{P_5} \right)^{\frac{\gamma-1}{\gamma}} - 1.0 \right] \right\}^{1/2}$$

$$V_5 = M_5 a_5$$

$$V_{z,5} = V_5 \cos \beta_5 = V'_{z,5}$$

$$V_{\theta,5} = V_5 \sin \beta_5$$

The various values relative to the rotor may also be determined from

$$V'_{\theta,5} = U - V_{\theta,5}$$

then

$$V'_5 = \sqrt{(V'_{z,5})^2 + (V'_{\theta,5})^2}$$

and

$$M'_5 = V'_5/a_5$$

$$P'_5 = P_5 \left[ 1 + \frac{\gamma-1}{2} (M'_5)^2 \right]^{\frac{\gamma}{\gamma-1}}$$

The angle of flow at the outlet with respect to the rotor may be calculated from

$$\beta'_5 = \sin^{-1} \frac{V'_{\theta,5}}{V'_5}$$

Passage recovery. An indication of loss in total pressure taking place in the rotor passage is given by the passage recovery factor, which is defined as

$$\text{Passage recovery} = \frac{P'_5}{P_2}$$

For a passage converging in the radial direction, the streamlines are assumed to converge uniformly and the blade relative total pressure is computed at the same relative position along the blade span at the inlet and the outlet.

## REFERENCES

1. **Kantrowitz, Arthur, and Donaldson, Coleman du P.:** Preliminary Investigation of Supersonic Diffusers. NACA ACR No. **L5D20**, 1945.
2. **Kantrowitz, Arthur:** The Supersonic Axial-Flow Compressor. NACA ACR No. **L6D02**, 1946.
3. Erwin, John R., Wright, **Linwood C., and Kantrowitz, Arthur:** **Investigation** of an Experimental Supersonic Axial-Flow **Compressor**. NACA **RM** No. **L6J01b**, 1946.
4. **Ritter, William K., and Johnsen, Irving A.:** Performance of **24-Inch** Supersonic Axial-Flow Compressor in Air. I - Performance of Compressor Rotor at Design Speed of 1600 Feet Per **Second**. NACA **RM** No. **E7L10**, 1946.

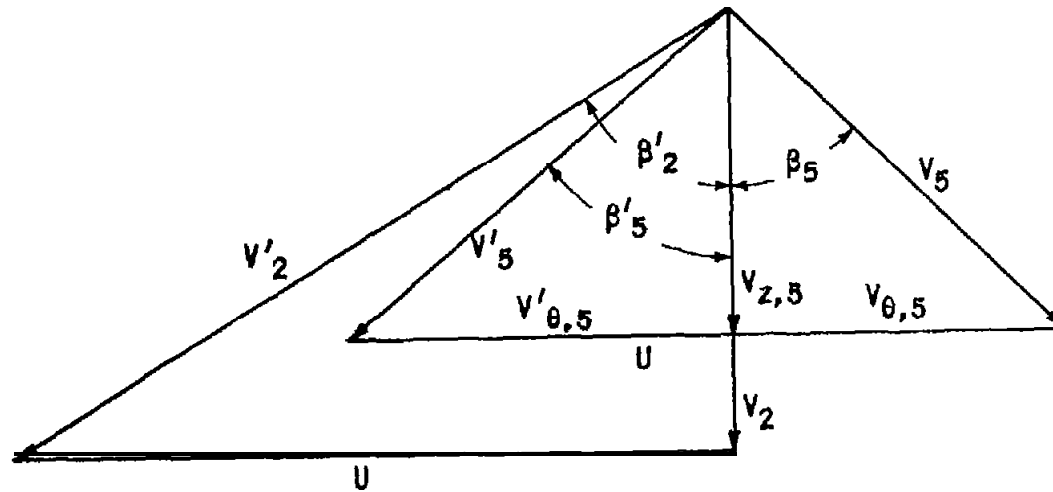


Figure 1. - Typical vector diagram for supersonic-compressor rotor without inlet guide vanes.

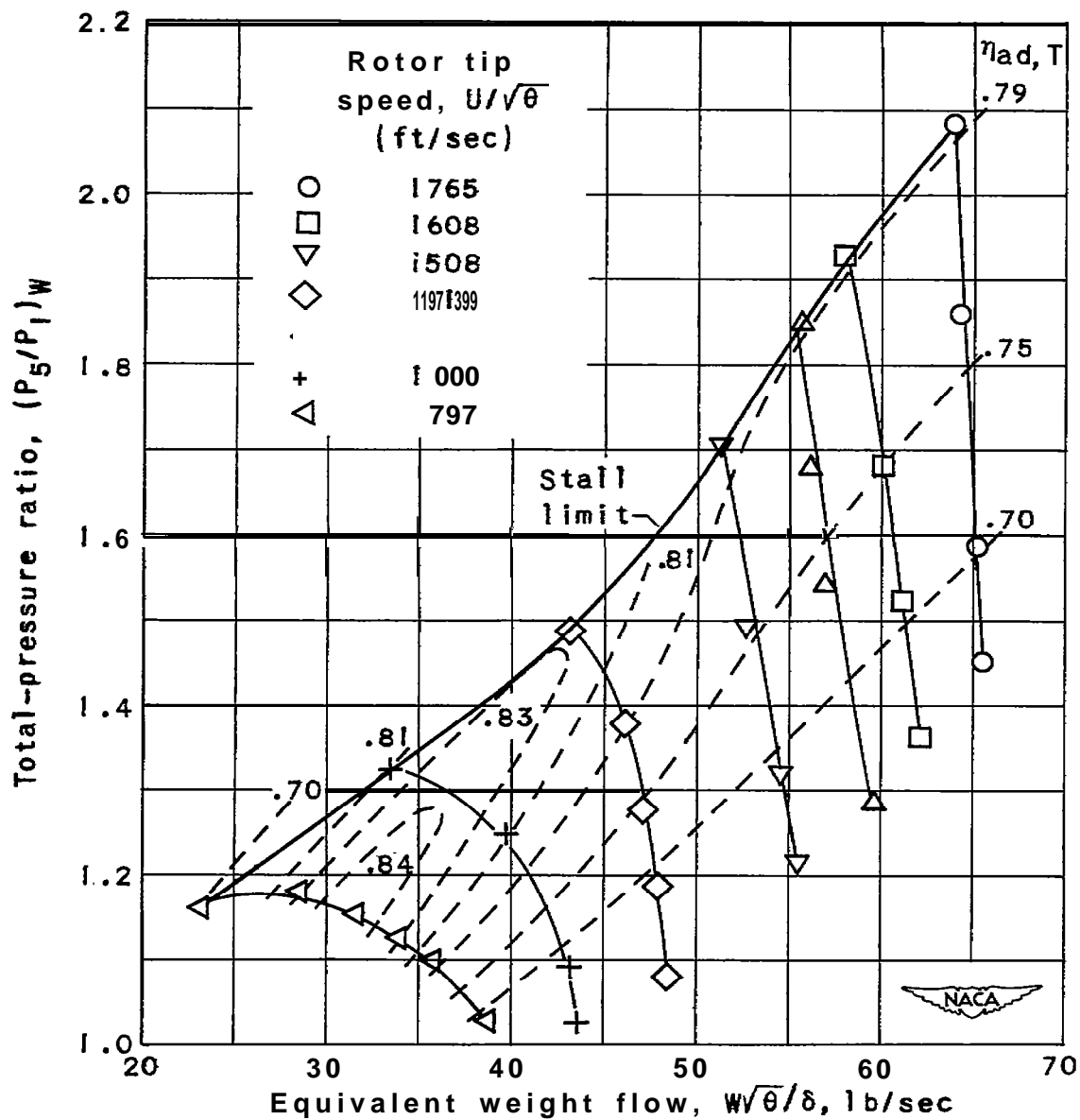


Figure 2. - Performance characteristics of 24-inch supersonic-compressor rotor.



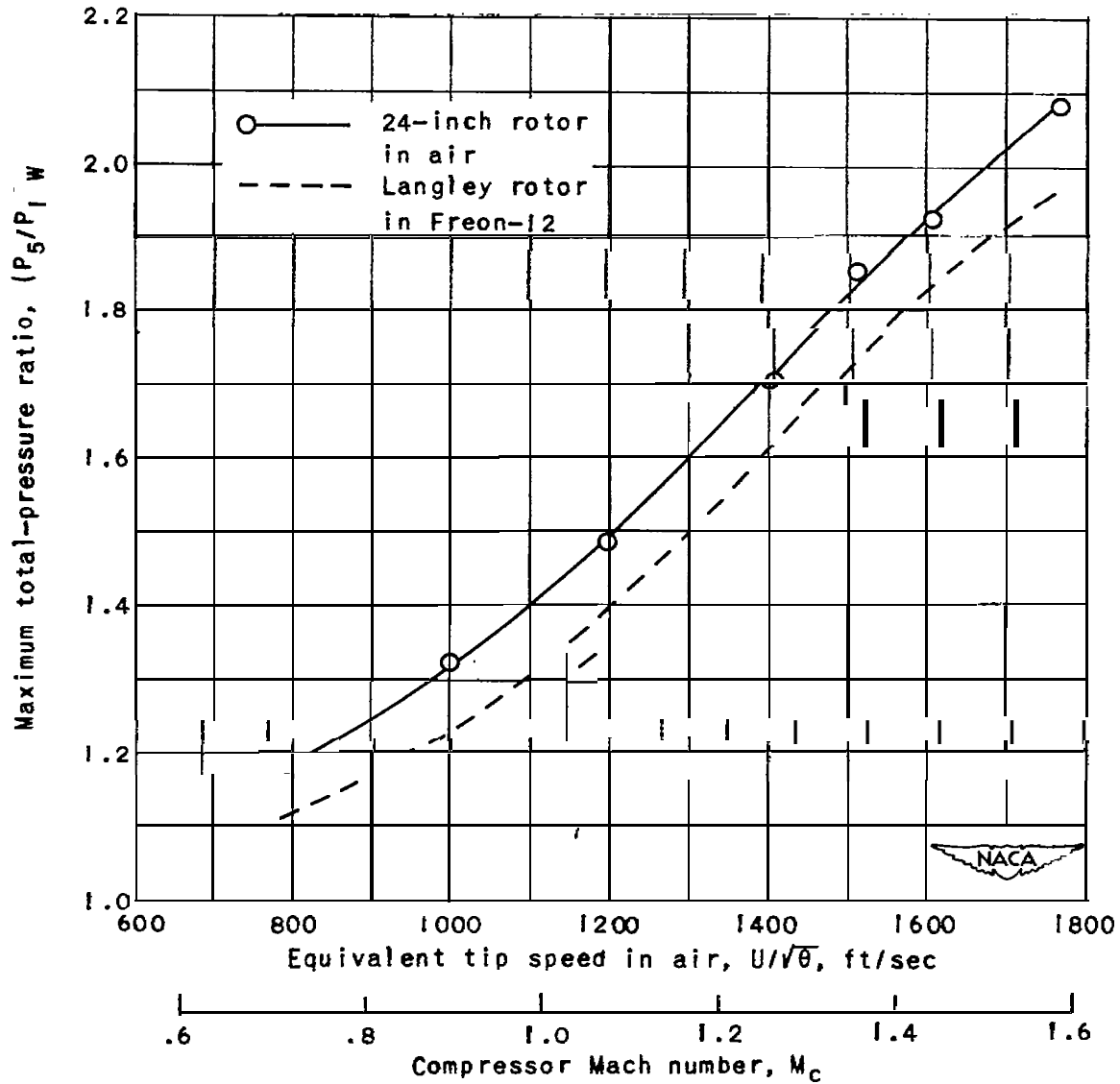


Figure 3. - Maximum total-pressure ratio of 24-inch supersonic-compressor rotor in air compared with results of Langley laboratory Freon-12 investigation (reference 3).

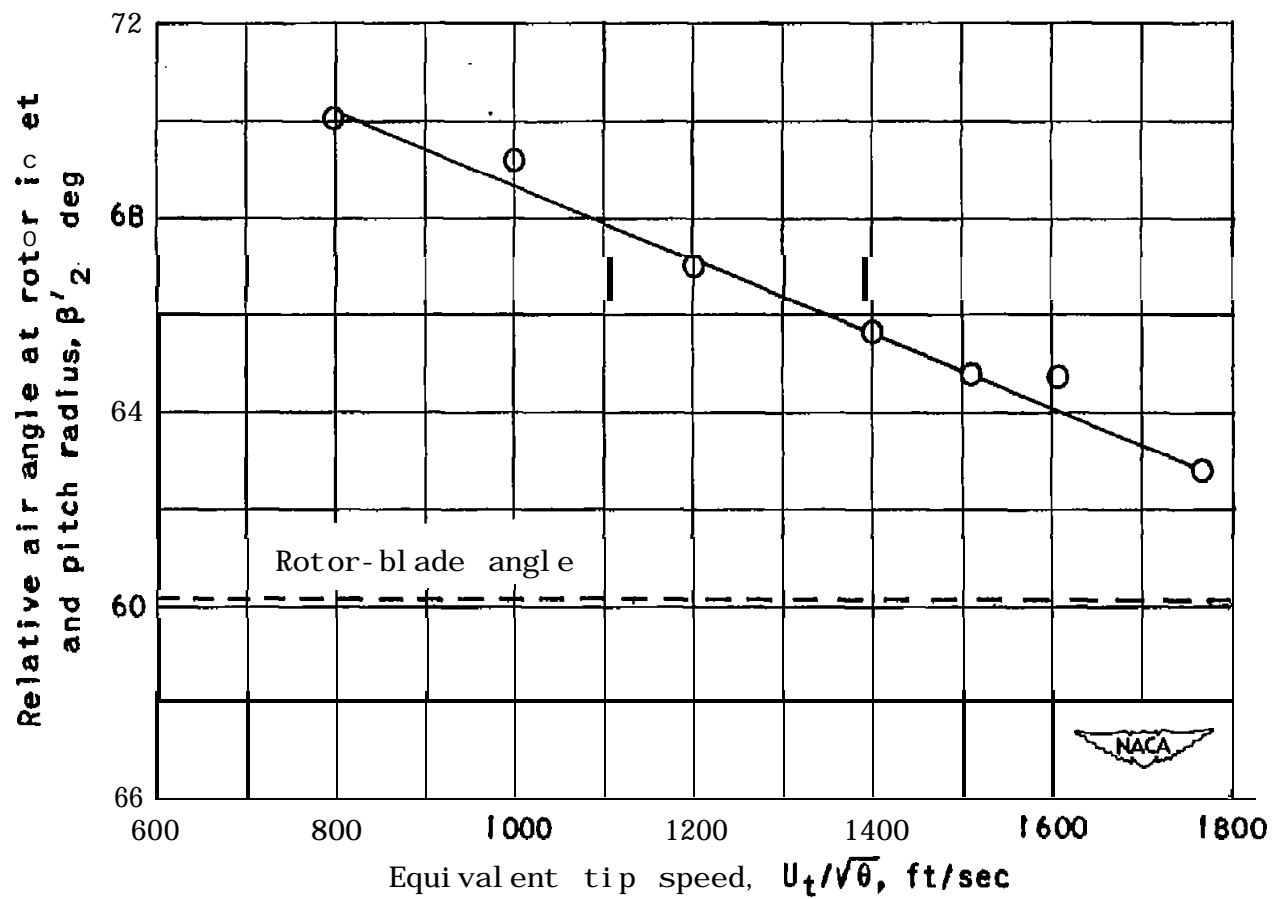


Figure 4. - Relative inlet air angle of 24-inch supersonic compressor under maximum total-pressure-ratio operation.

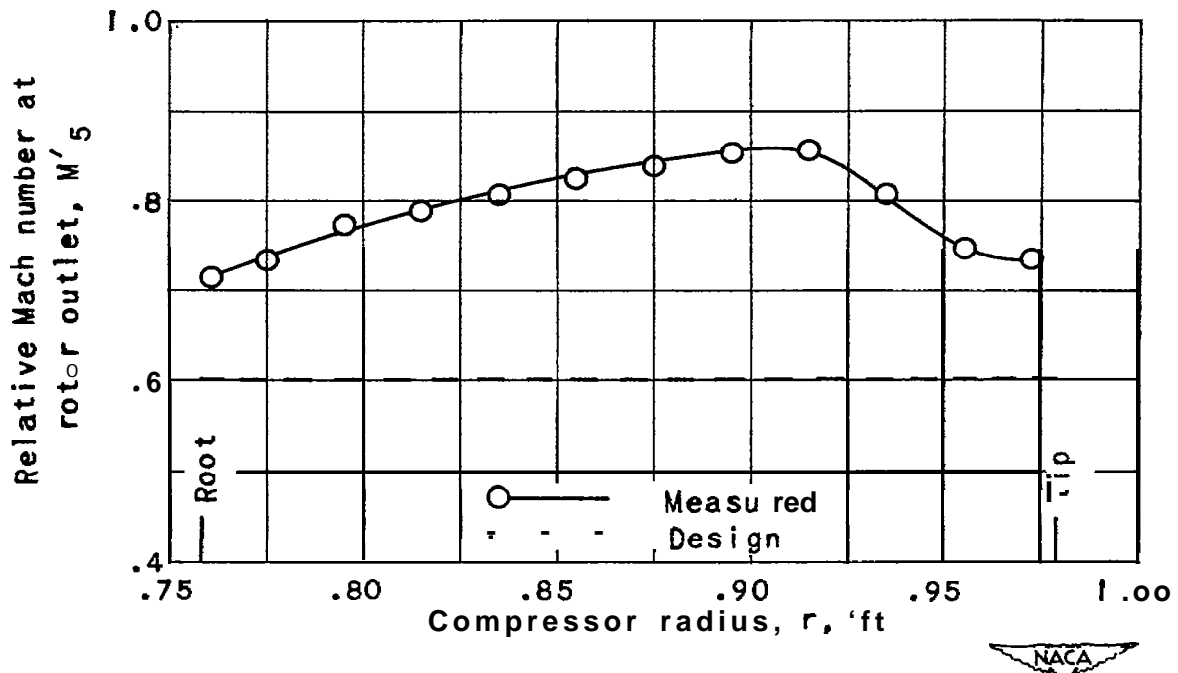


Figure 5. - Relative Mach number profile of 24-inch supersonic-compressor rotor. Maximum pressure-ratio condition at equivalent tip speed of 1608 feet per second.

997

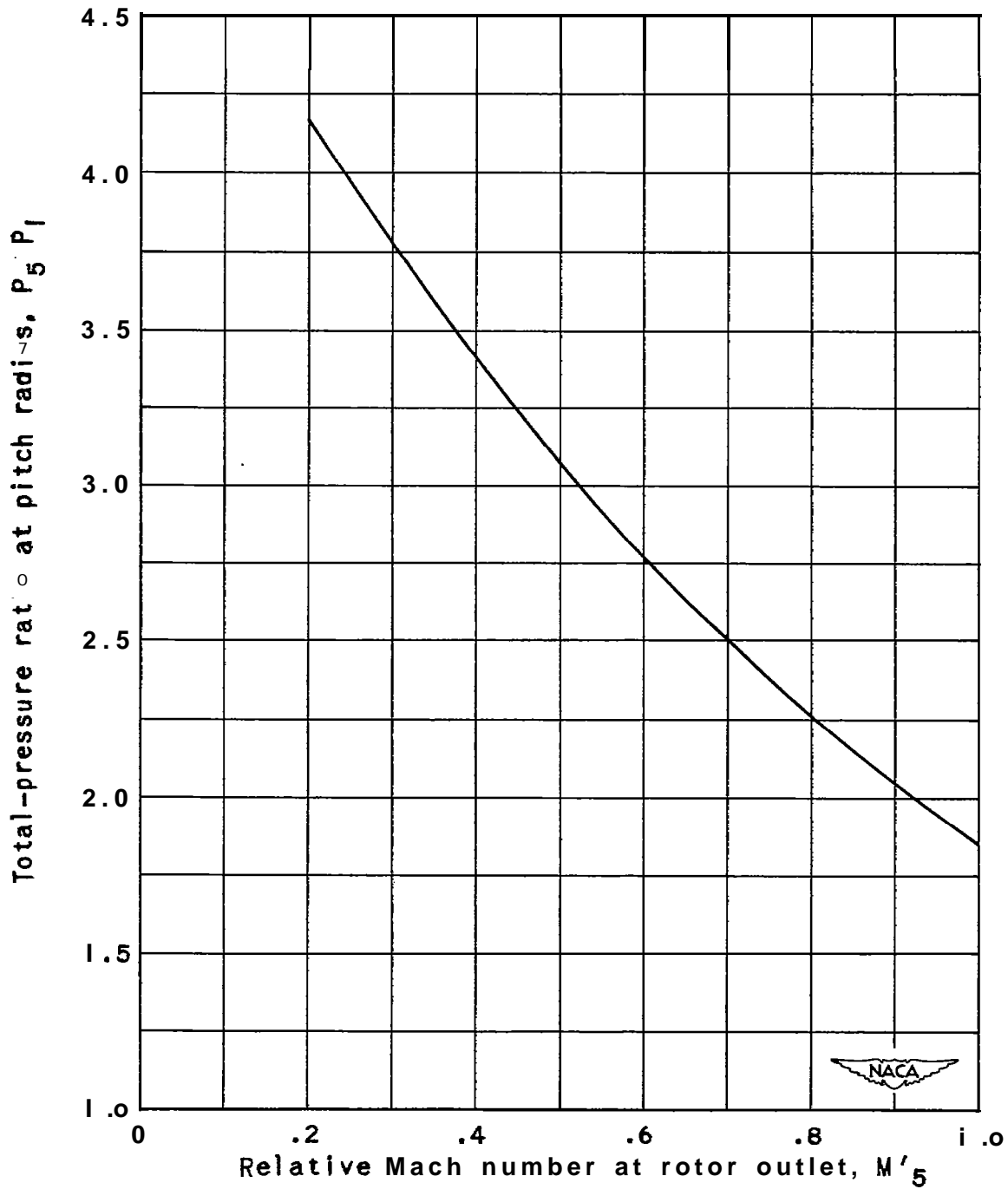


Figure 6. - Variation of calculated total-pressure ratio at tip speed of 1600 feet per second with relative Mach number at rotor outlet,

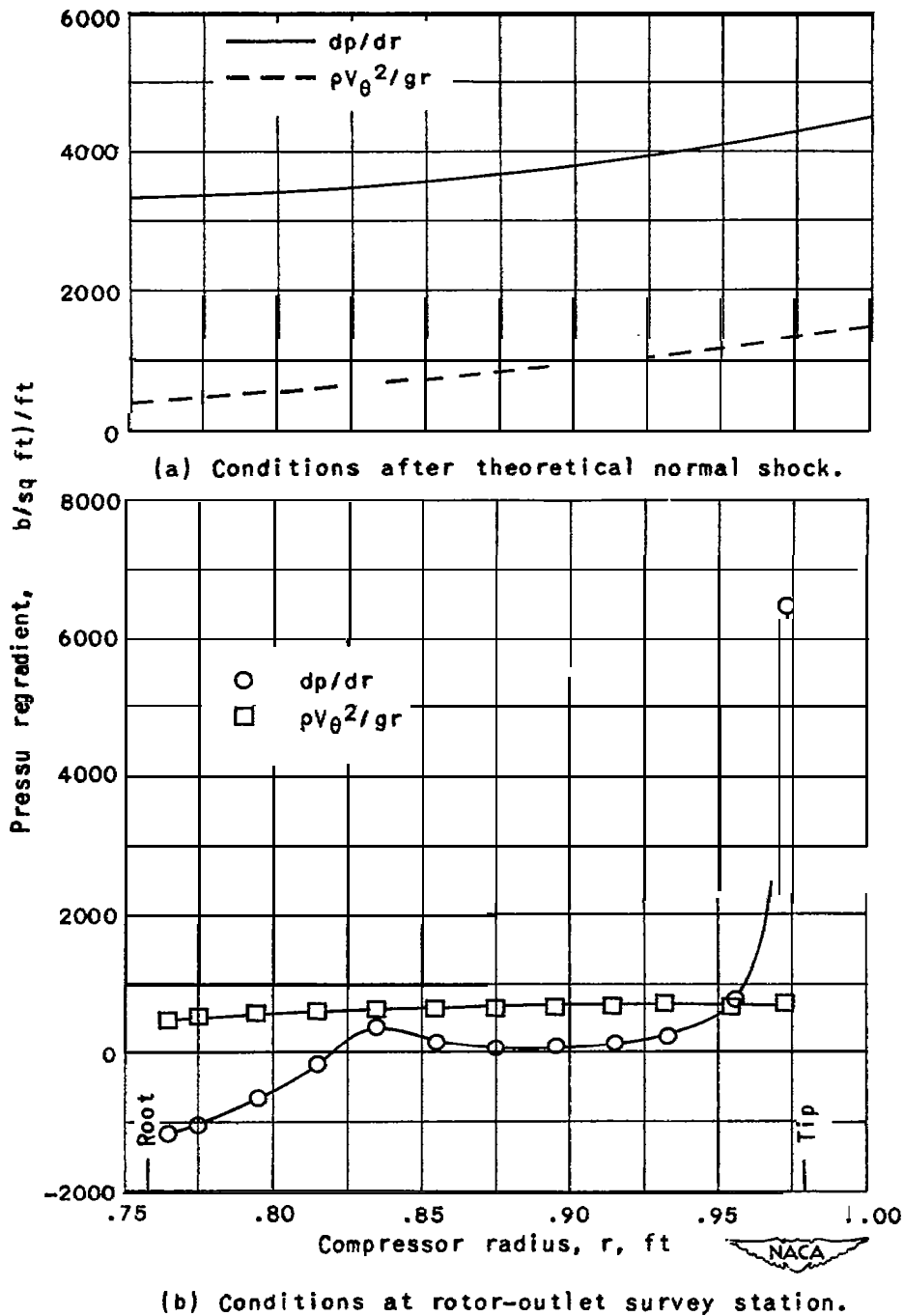


Figure 7. - Pressure gradients after normal shock and at rotor-outlet survey station of 24-inch supersonic-compressor rotor. Maximum pressure-ratio condition at equivalent tip speed of 1608 feet per second.

997

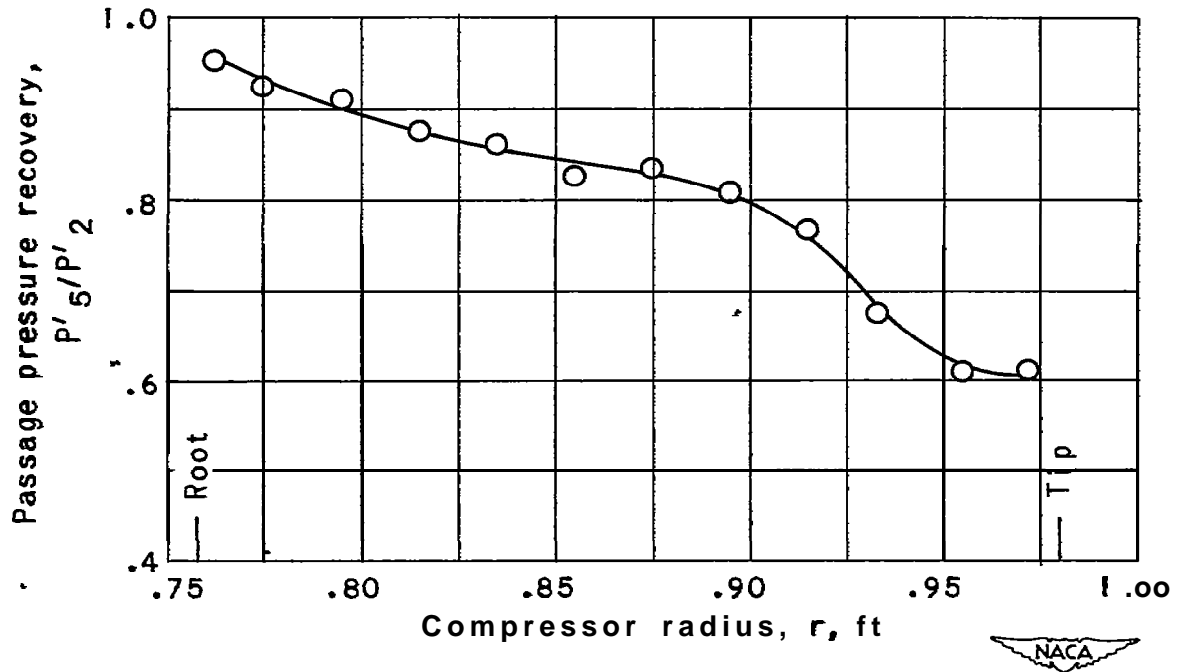


Figure 8. - Passage pressure recovery of 24-inch supersonic-compressor rotor. Maximum pressure-ratio condition at equivalent tip speed of 1608 feet per second.

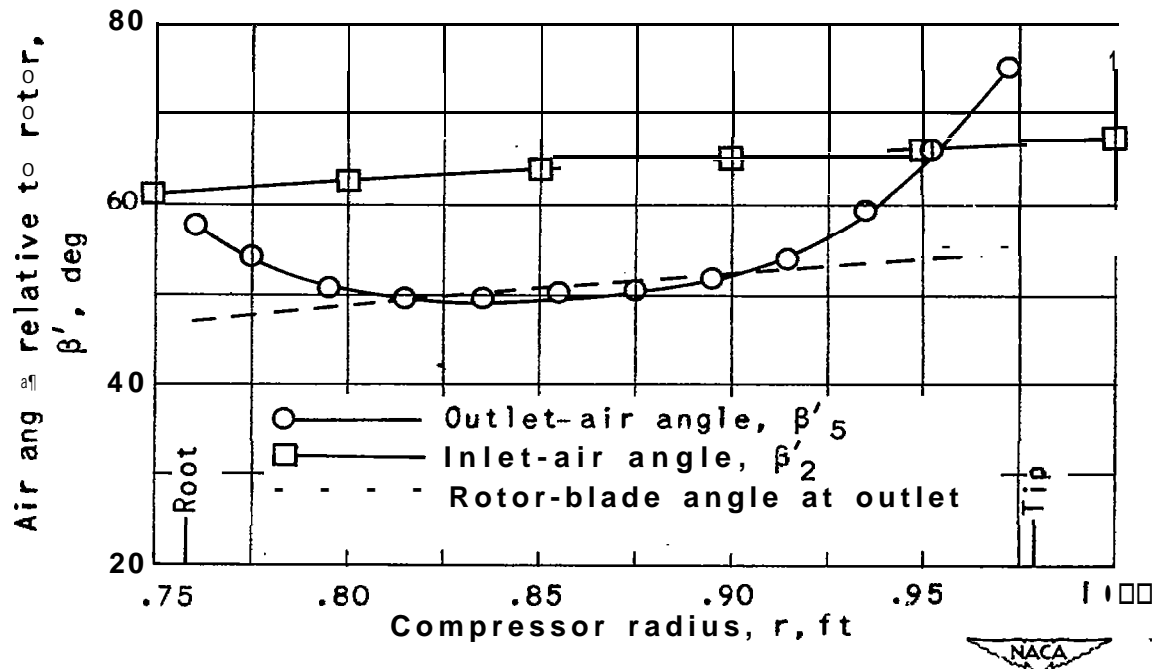


Figure 9. - Relative air-angle profile of 24-inch supersonic-compressor rotor. Maximum pressure-ratio condition at equivalent tip speed of 1608 feet per second.

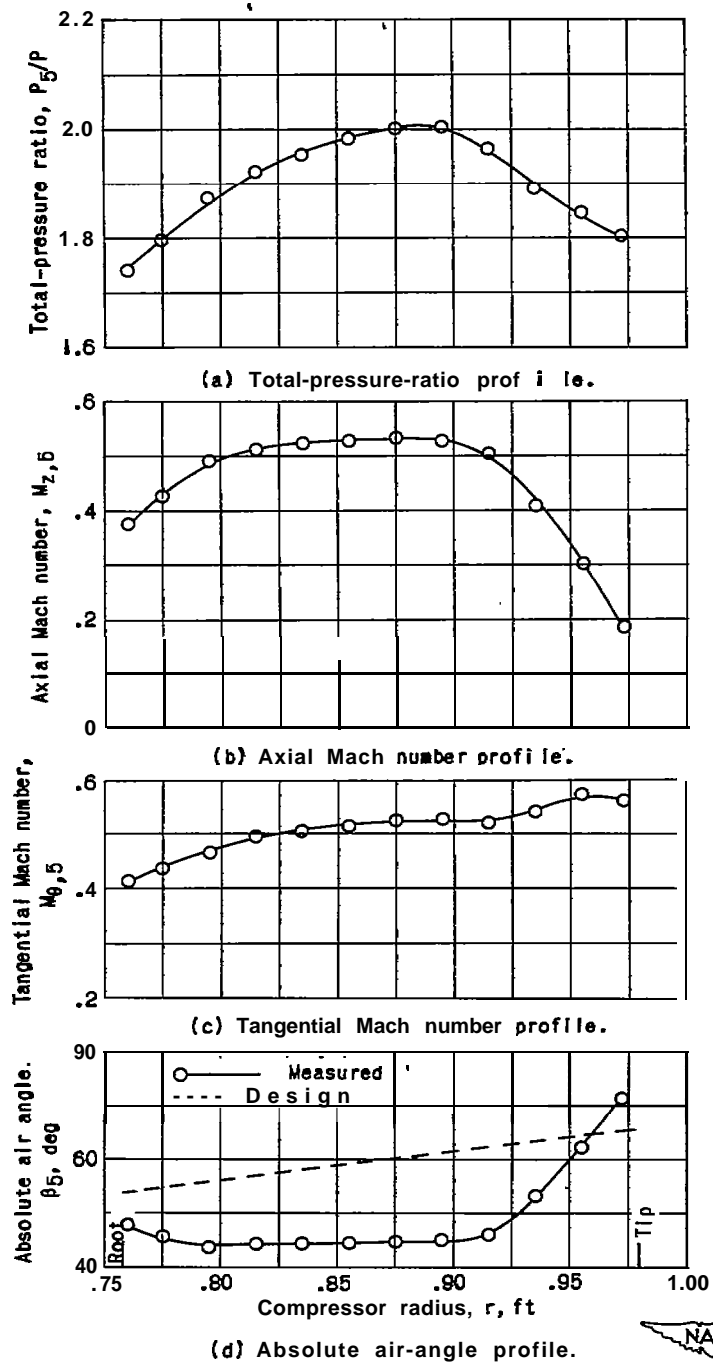


Figure 10. - Total-pressure ratio, axial and tangential Mach numbers, and absolute air-angle profiles of 24-inch supersonic-compressor rotor at rotor outlet. Maximum pressure-ratio condition at equivalent tip speed of 1608 feet per second.



NASA Technical Library



3 1176 01435 5458

